Hawke's Bay 3D Aquifer Mapping Project:

Heretaunga Plains numerical groundwater model updates using SkyTEM data

January 2024
Hawkes Bay Regional Council Publication No. 5632

HAWKES BAY
REGIONAL COUNCIL
TE KAUNIHERA Ā-ROHE O TE MATAU-A-MĀUI

ISSN 2703-2051 (Online)
ISSN 2703-2043 (Print)

HAWKES BAY REGIONAL COUNCIL
TE KAUNIHERA Ā-ROHE O TE MATAU-A-MĀUI

(06) 835 9200
0800 108 838
Private Bag 6006 Napier 4142
159 Dalton Street . Napier 4110

Environmental Science

Hawke's Bay 3D Aquifer Mapping Project:

Heretaunga Plains numerical groundwater model updates using SkyTEM data

January 2024
Hawkes Bay Regional Council Publication No. 5632

Prepared By:
GNS Science
ZJ Rawlinson BJC Hemmings CR Moore

For: Hawke's Bay Regional Council

Reviewed by:
SG Cameron, GNS Science

ISSN 2703-2051 (Online)
ISSN 2703-2043 (Print)

.

30 January 2024

Team Leader – Hydrology and Groundwater Science
Hawke's Bay Regional Council
Private Bag 6006
Napier 4142

Attention: Simon Harper

Wairakei Research Centre
114 Karetoto Road
RD 4
Taupō 3384
Private Bag 2000
Taupō Mail Centre
Taupō 3352
New Zealand
T +64-7-374 8211
F +64-4-570 4600
www.gns.cri.nz

Dear Simon,

Hawke's Bay 3D Aquifer Mapping Project: Heretaunga Plains numerical groundwater model updates using SkyTEM data

1.0 SUMMARY

As part of the Hawke's Bay 3D Aquifer Mapping Project (3DAMP), this report focuses on an update of the Heretaunga Plains numerical groundwater model (Figure 1.1) using SkyTEM-derived models.

The model used is the steady-state Heretaunga Plains numerical groundwater model (Heretaunga GW model) developed as part of the GNS-Science-led Te Whakaheke o Te Wai (TWOTW) Ministry of Business, Innovation & Employment (MBIE) Endeavour Programme. This model used a 3D geological model (Begg et al. 2022) as its primary base for defining model layers and properties. The Heretaunga GW model was updated primarily with SkyTEM-derived hydrogeological interpretation models developed in Rawlinson (2023).

The following model parameters (initial values and prior distributions) were updated: hydraulic conductivity (horizontal and vertical), streambed hydraulic conductivity, drain conductances, and porosity. Additional parameters defined on the basis of hydraulic conductivity were also modified. These include general head boundary (GHB) conductances around the inland boundary of the model. The following model structures were updated: model layering and depth to basement.

Figures herein highlight the differences between the two models. The updated Heretaunga GW model contains significantly greater property variation over short spatial scales, owing to the high spatial resolution of the SkyTEM data. The extent of the modification of prior parameter distributions (means and standard deviations) varies over the mapped area, with SkyTEM data reducing prior standard deviations in some locations and increasing it in others.

More detailed explorations of the implications of these modifications on model simulated prediction uncertainties and prior parameter distribution definitions will be undertaken in a subsequent piece of work.

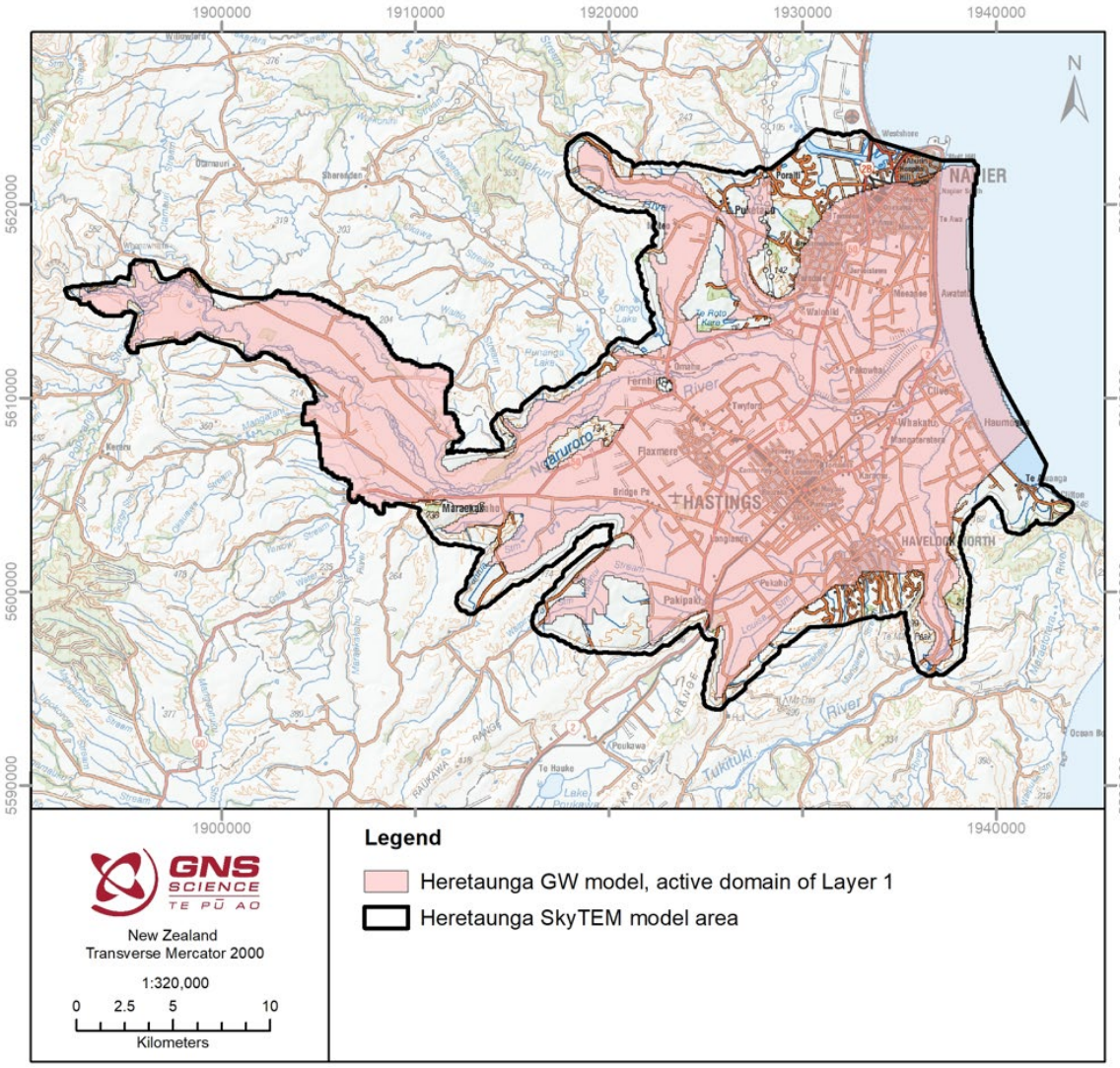

Figure 1.1 Heretaunga GW model area, shown as the active domain of Layer 1. Also shown for comparison is the Heretaunga SkyTEM model area (extent of the 3D models derived from the SkyTEM data).

2.0 MODEL UPDATES

2.1 Parameter Updates

The central-mode (mean) of prior parameter distributions were updated on the basis of insights from SkyTEM data. Mean values of prior parameter distributions for horizontal hydraulic conductivity (KH), vertical hydraulic conductivity (KV), stream bed hydraulic conductivity, drain conductance and porosity have been modified. The updates of model parameters are described in Table 2.1 and shown in Figures 5.1–5.3. The magnitude of parameter log variance was kept consistent between the models; however, the individual parameter value ranges covered by the prior distributions (which define prior uncertainty) change as a function of the change in mean value.

While there is an established context for relating SkyTEM information (electrical conductivity based) to hydraulic conductivity (e.g. Purvance and Andricevic 2000), the relationship between SkyTEM-derived information and porosity is less well established. This is especially the case where clay is present in mixed sediment aquifers and application of Archie's Law is not valid (Purvance and Andricevic 2000). For mixed sediment aquifers, such as in the Heretaunga Plains, porosity is likely to be influenced by the degree of fine material (especially clay). We anticipate that the SkyTEM-derived coarse-fraction classification model ('CC' model; Rawlinson 2023) provides some quantity to relate to porosity of mixed sediments. However, we expect this relationship to be complex and non-linear. The following describes the translation from SkyTEM-derived CC to updated mean values of prior distributions of porosity.

We compared porosity estimates from previous studies (Tonkin & Taylor 2016, 2018) to the SkyTEM-derived CC model (Rawlinson 2023) values at a number of wells in the area. These 'data' points were supplemented by additional observations in similar mixed sediment systems. Open framework gravels make up about 13–17% of highly conductive mixed alluvial sediments (e.g. Burbery et al. 2018; Moore et al. 2022), and this highly conductive mix corresponds to the highest CC values (CC = 1.0). Counter-intuitively, effective porosity of these units has been observed to be low, on the order of 0.003 (e.g. Thorpe et al. 1982; Dann et. al. 2008), due to the relatively low percentage of the highly permeable connected open framework gravels. In contrast, Pang et al. (1998) estimated a porosity of 0.2 in alluvial gravel strata in Burnham, which we have hypothesised to correspond to intermediate CC values. These observations and estimates (red crosses in Figure 2.1) provide anchors for a parametric curve fitting (black line in Figure 2.1), which in turn provides the basis for translating from CC to mean values for porosity probability distributions.

Some additional adjustments were also undertaken. The CC model places interpreted consolidated sediments (hydrogeological basement) to CC values between 0.001 and 0.014 (see Rawlinson [2023]). For these consolidated sediments, porosity was set to 0.05. For lower layers (layers 7–9), the porosity decline at low and high CC values was subdued (orange dots in Figure 2.1). This results in slightly less variation in porosity with CC in the deeper layers compared to the upper layers (blue dots in Figure 2.1). Finally, a lower limit of 0.003 was enforced. The lower limit and depth adjustment to mean values of porosity prior distributions are consistent with the original model. The total range in prior distribution mean values across the model domain is 0.003–0.15.

Porosity is a highly uncertain parameter within numerical models, and the relationship derived here is also considered highly uncertain. This uncertainty is propagated through the model through the specification of high prior variances and will be explored in ongoing work. As with the other hydraulic properties (e.g. KH and KV), the inference of model cell-scale porosity from SkyTEM-derived information is likely to evolve as our understanding of the scale-dependent material property, and feature, controls on electrical and hydraulic properties improves.

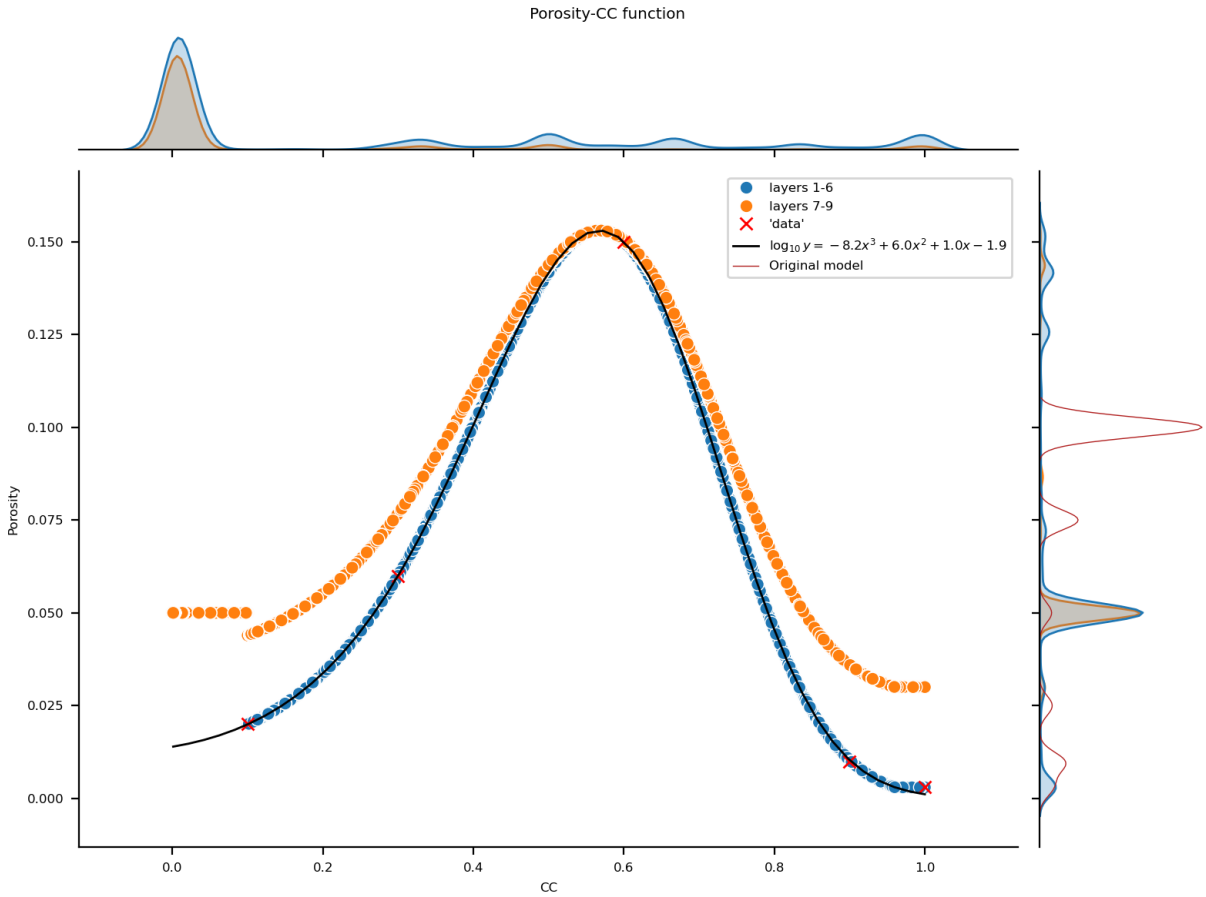

Figure 2.1 The relationship derived for translating SkyTEM-derived CC to mean values for porosity parameter distributions. 'Data' points detail the low porosity values expected at both high CC (open framework gravels) and low CC (clay-rich). Marginal plots indicate frequency of CC and porosity values in model cells. The original model used a default value of 0.1.

Table 2.1 Update of Heretaunga GW model parameters.

Parameter	Original Initial Value Source ('geo')	Updated Initial Value Source ('skytem')
KH	Uniform values based on literature values and expert knowledge set to different geological model units (Begg et al. 2022). Low KH buffer added to basin edges in order to enable model to fit to tritium data. Lower KH added to the western extent of the Ngaruroro River in order to fit to groundwater levels. Geological model did not extend offshore; uniform values set based on expectation of confining layer extension in layer 1, gravel layers in layers 2–6 and medium permeability geology in layers 7–9.*	SkyTEM-derived estimates of KH (geometric mean, clipped to a minimum of 5×10^{-4} m/day): *KH_initial_basehigh* model (Rawlinson 2023)
KV	Uniform KV/KH ratios based on literature values and expert knowledge set to different geological model units (Begg et al. 2022).	SkyTEM-derived estimates of coarse-fraction (CC model; Rawlinson 2023) and KH (*KH_initial_basehigh* model; Rawlinson 2023) converted to KV. $KV = KH*10^{(4*CC)-4}$. Assumed minimum value of $KH*10^{-4}$. (Vertical anisotropy assumed to have a log-linear relationship to clay content.)
Streambed hydraulic conductivity	Values based on KV of layer 1, with linear scaling adjustment between assumed minimum and maximum values (0.01 and 200 m/day, respectively).	Calculated same as KV but using the upper 4 m of the SkyTEM-derived models (arithmetic mean of CC and geometric mean of *KH_initial_basehigh*; Rawlinson 2023), with linear scaling adjustment between assumed minimum and maximum values (0.01 and 200 m/day, respectively).
Drain conductances	Values based on KV of layer 1, with adjustment to convert to conductance (using cell dimensions and thickness) and linear scaling adjustment between assumed minimum and maximum values (10 and 2×10^5 m^2/day, respectively).	Calculated same as KV but using the upper 4 m of the SkyTEM-derived models (arithmetic mean of CC and geometric mean of *KH_initial_basehigh*; Rawlinson 2023), with adjustment to convert to conductance (using cell dimensions and thickness) and linear scaling adjustment between assumed minimum and maximum values (10 and 2×10^5 m^2/day, respectively).
Porosity	Uniform values based on literature values and expert knowledge set to different geological model units (Begg et al. 2022). Low-porosity buffer added to basin edges in order to enable model to fit to tritium data. Default value of 0.1 used. See text for further details.	SkyTEM-derived estimates of coarse-fraction (CC model; Rawlinson 2023) used to estimate porosity. Porosity assumed to have a non-linear relationship with coarse-fraction. See text and Figure 2.1 for further details.

* This assumption applied to all original model parameters.

2.2 Structure Updates

The updates of model structures are described in Table 2.2 and shown in Figures 5.3 and 5.4.

Table 2.2 Update of Heretaunga GW model structures.

Structure	Original Source ('geo') (Begg et al. 2022)	Updated Source ('skytem') (Sahoo et al. 2023; Rawlinson 2023)	Comment
Model Layers L1–L3	Heretaunga Formation	HU = 1	Minimum thickness (6 m base of L3) set where non-existent.
Model Layers L4–L6	Maraekakaho Formation and riverbed and river mouth gravels	HU = 2	Minimum thickness (45 m base of L6) set where non-existent.
Model Layers L7–L9	Early to middle Pleistocene	HU = 3	Minimum thickness (120 m base of L9) set where non-existent.
Basement	Undifferentiated Paleocene–Pleistocene	HU = 4	Cut-off set at -270 m below sea level.

3.0 RESULTS OF UPDATED PRIORS

Changes in prior distributions as a consequence of the model updates are shown in Figures 5.5–5.9. Mapped means and standard deviations of prior distributions highlight that changes are variable across the model area. Violin plots highlight the changes in prior distributions for select outputs. The SkyTEM data reduced prior standard deviations in some areas but increased it in others. These variations are related to the quality of existing datasets, as well as to the (non)linearity of the relationship between parameter values and simulated outputs across parameter space. Subsequent work is exploring the addition of using SkyTEM data to inform parameter variances (uncertainty) (i.e. not just informing the mean values of parameter distributions). The propagation of uncertainty to posterior distributions (after history-matching) and the impact of the SkyTEM data in this process will also be explored in a subsequent piece of work.

Yours sincerely,

Zara Rawlinson
Senior Hydro-Geophysicist

Brioch Hemmings
Senior Groundwater Modeller

Catherine Moore
Principal Groundwater Modeller

4.0 ACKNOWLEDGEMENTS

This work has been jointly funded by the New Zealand Government's Provincial Growth Fund, Hawke's Bay Regional Council and GNS Science's Strategic Science Investment Fund (MBIE).

5.0 REFERENCES

Begg JG, Jones KE, Lee JM, Tschritter C. 2022. 3D geological map of the Napier-Hastings urban area [explanatory text]. Lower Hutt (NZ): GNS Science. 21 p. (GNS Science geological map; 7b). https://doi.org/10.21420/QFEK-9369

Burbery LF, Moore CR, Jones MA, Abraham PM, Humphries BL, Close ME, Ventra D, Clarke LE. 2018. Study of connectivity of open framework gravel facies in the Canterbury Plains aquifer using smoke as a tracer. In: Ventra D, Clarke LE, editors. *Geology and geomorphology of alluvial and fluvial fans: terrestrial and planetary perspectives*. London (GB): Geological Society of London. p. 327–344. (Geological Society of London special publications; 440). https://doi.org/10.1144/SP440.10

Dann RL, Close ME, Pang L, Flintoft MJ, Hector RP. 2008. Complementary use of tracer and pumping tests to characterize a heterogeneous channelized aquifer system in New Zealand. *Hydrogeology Journal*. 16(6):1177–1191. https://doi.org/10.1007/s10040-008-0291-4

Moore C, Scott D, Burbery L, Close M. 2022. Using sequential conditioning to explore uncertainties in geostatistical characterization and in groundwater transport predictions. *Frontiers in Earth Science*. 10. https://doi.org/10.3389/feart.2022.979823

Pang L, Close M, Noonan M. 1998. Rhodamine WT and *Bacillus subtilis* transport through an alluvial gravel aquifer. *Groundwater*. 36(1):112–122. https://doi.org/10.1111/j.1745-6584.1998.tb01071.x

Purvance DT, Andricevic R. 2000. On the electrical-hydraulic conductivity correlation in aquifers. *Water Resources Research*. 36(10):2905–2913. https://doi.org/10.1029/2000WR900165

Rawlinson ZJ. 2023. Hawke's Bay 3D aquifer mapping project: 3D hydrogeological models from SkyTEM data in the Heretaunga plains. Lower Hutt (NZ): GNS Science. 77 p. Consultancy Report 2023/57. Prepared for Hawke's Bay Regional Council.

Sahoo TR, Rawlinson ZJ, Kellett RL. 2023. Hawke's Bay 3D Aquifer Mapping Project: delineation of major hydrological units within the Heretaunga Plains from SkyTEM-derived resistivity models. Lower Hutt (NZ): GNS Science. 55 p. Consultancy Report 2022/30. Prepared for Hawke's Bay Regional Council.

Thorpe HR, Burden RJ, Scott DM. 1982. Potential for contamination of the Heretaunga Plains aquifers. Christchurch (NZ): Ministry of Works and Development. 148 p. Water and Soil Technical Publication 24.

Tonkin & Taylor. 2016. Bacterial contamination investigation. [Place unknown] (NZ): Tonkin & Taylor Ltd. Job 31301.100. Prepared for Hastings District Council.

Tonkin & Taylor. 2018. Source protection zones for public supply bores: Hastings urban area. [Napier] (NZ): Tonkin & Taylor Ltd. 65 p. Report 1005769. Prepared for Hastings District Council.

FIGURES

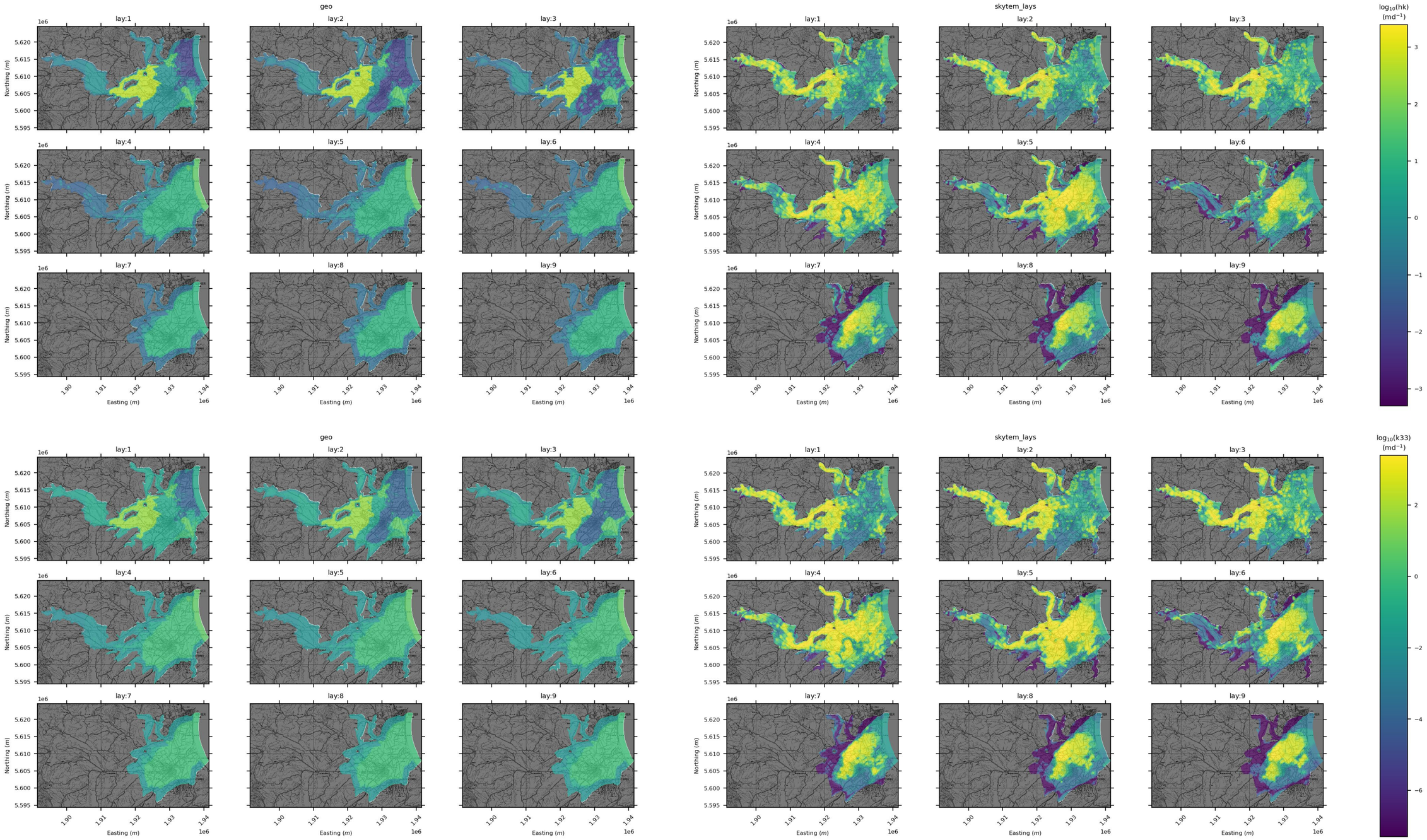

Figure 5.1 (Top) Horizontal hydraulic conductivity (m/day). (Bottom) Vertical hydraulic conductivity (m/day). (Left) Original model. (Right) Updated model. Layers (lay) 1–9 of the model are shown.

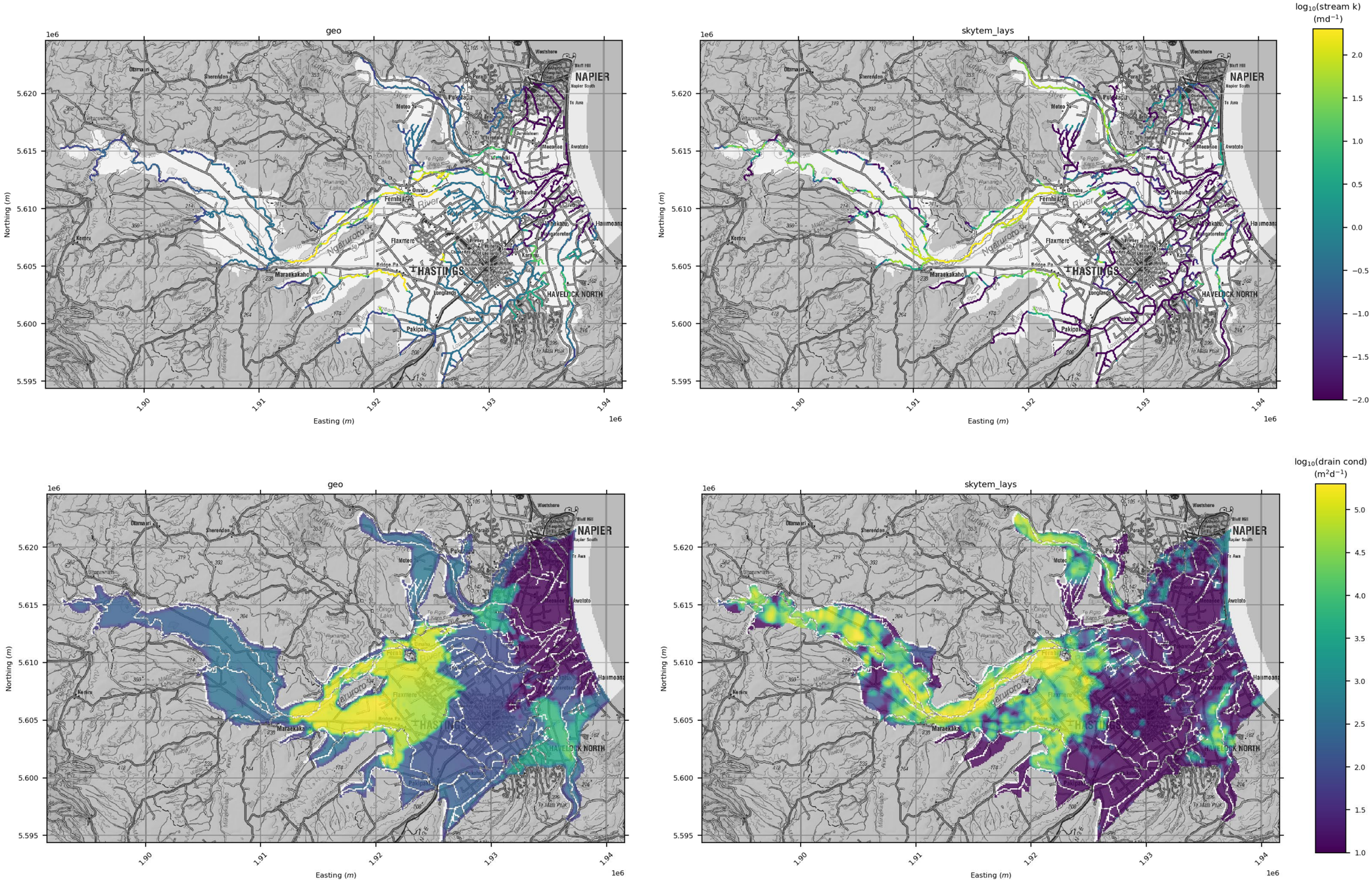

Figure 5.2 (Top) Stream hydraulic conductivity (m/day). (Bottom) Drain conductances (m^2/day). (Left) Original model. (Right) Updated model. These parameters are only active in layer 1 of the model.

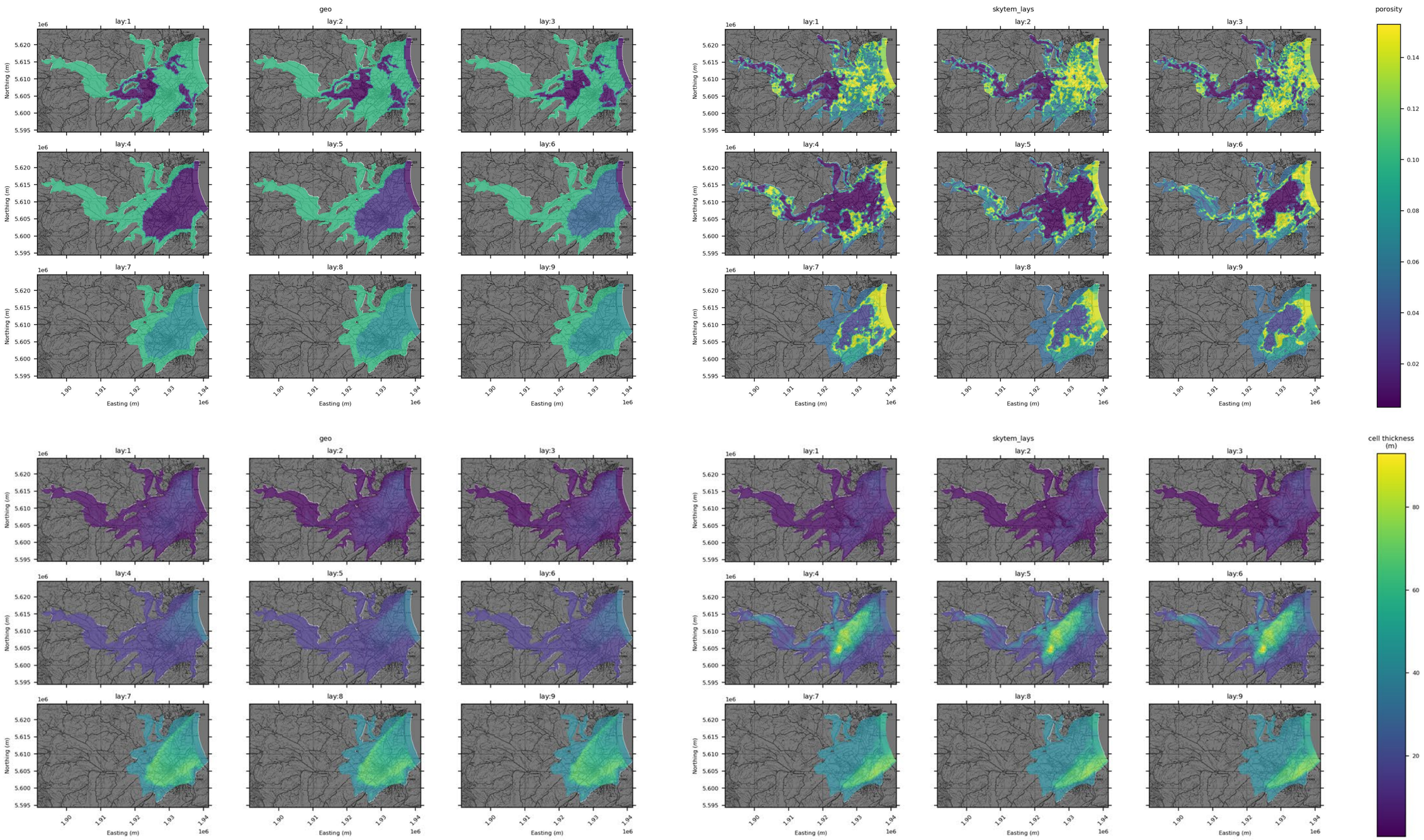

Figure 5.3 (Top) Porosity. (Bottom) Layer thicknesses (m). (Left) Original model. (Right) Updated model. Layers (lay) 1–9 of the model are shown.

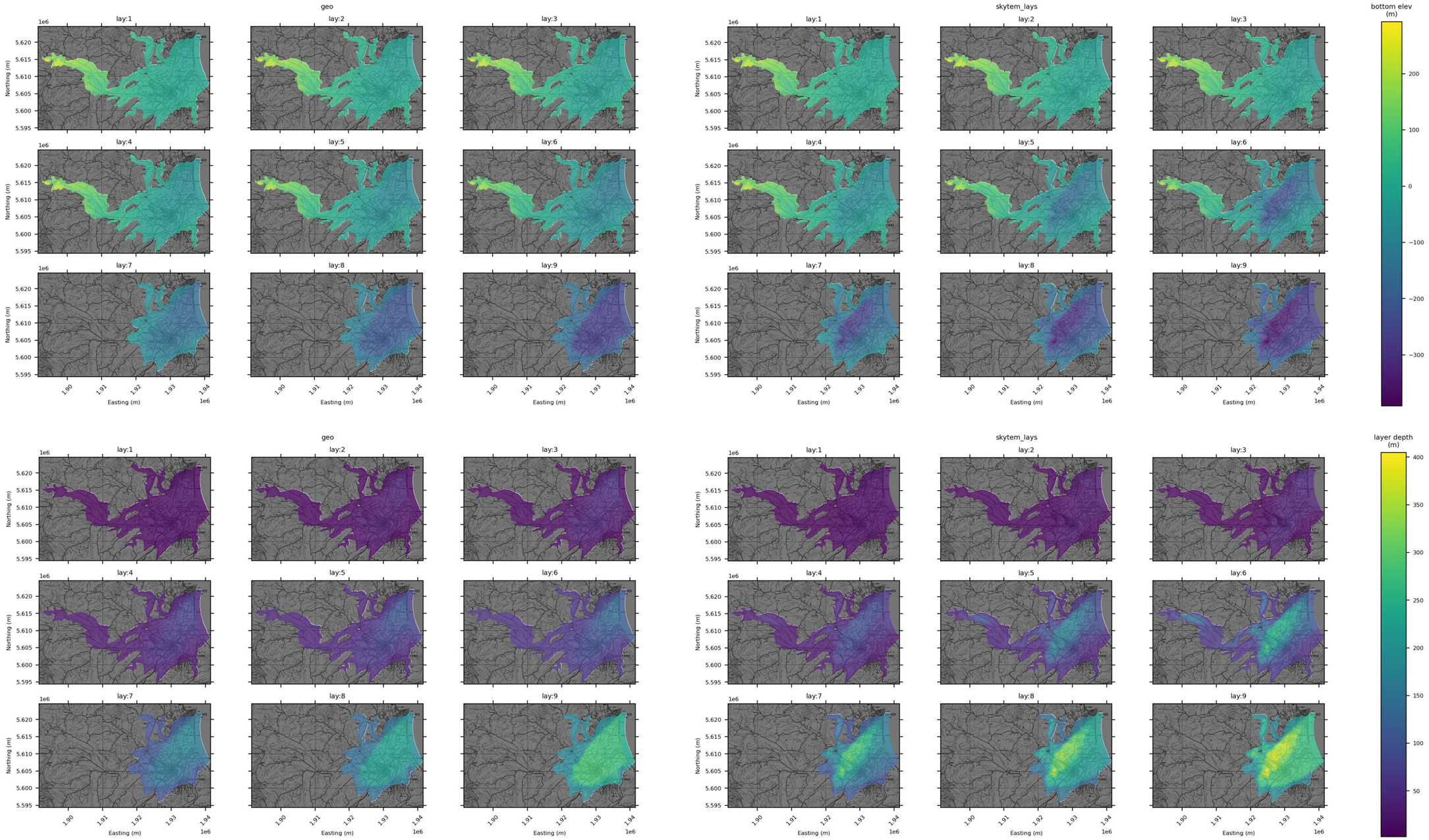

Figure 5.4 (Top) Layer bottom elevations (metres above sea level). (Bottom) Layer bottom depths (m). (Left) Original model. (Right) Updated model. Layers (lay) 1–9 of the model are shown.

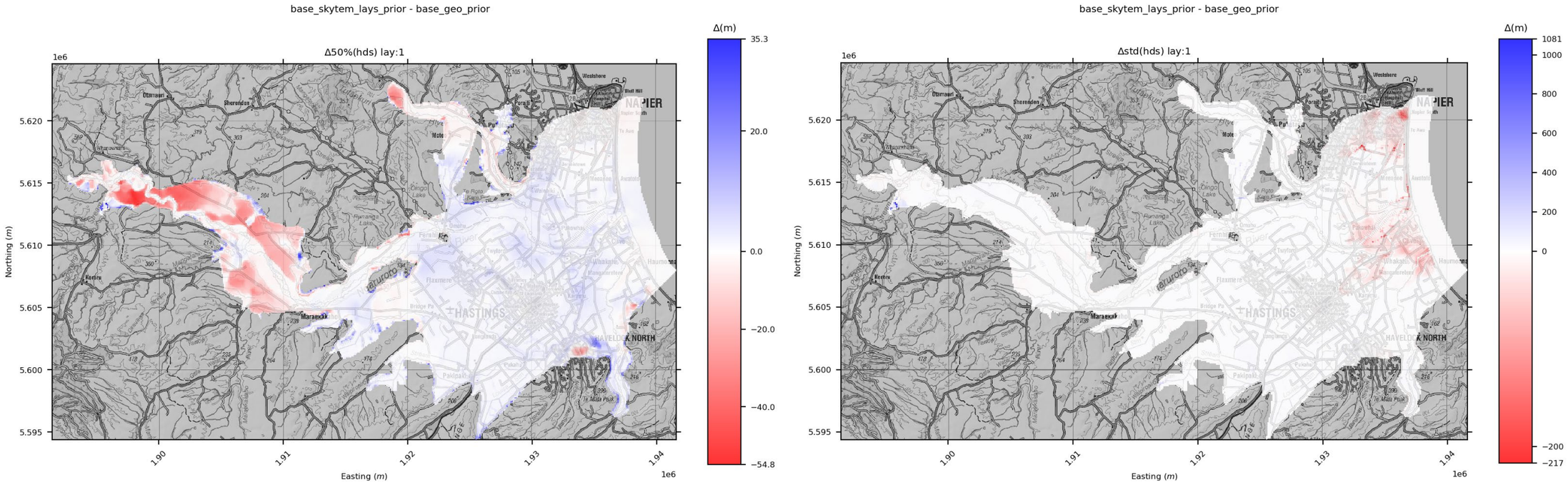

Figure 5.5 Change in simulated groundwater level (head) prior ensemble median (left) and standard deviation (right) for the updated model compared to the original model. Blue colours in the left-hand plot indicate an increase in the ensemble median simulated groundwater level for the updated model. For the right-hand plot, red colours indicate decreases in prior ensemble standard deviation (variance/uncertainty) in the updated model.

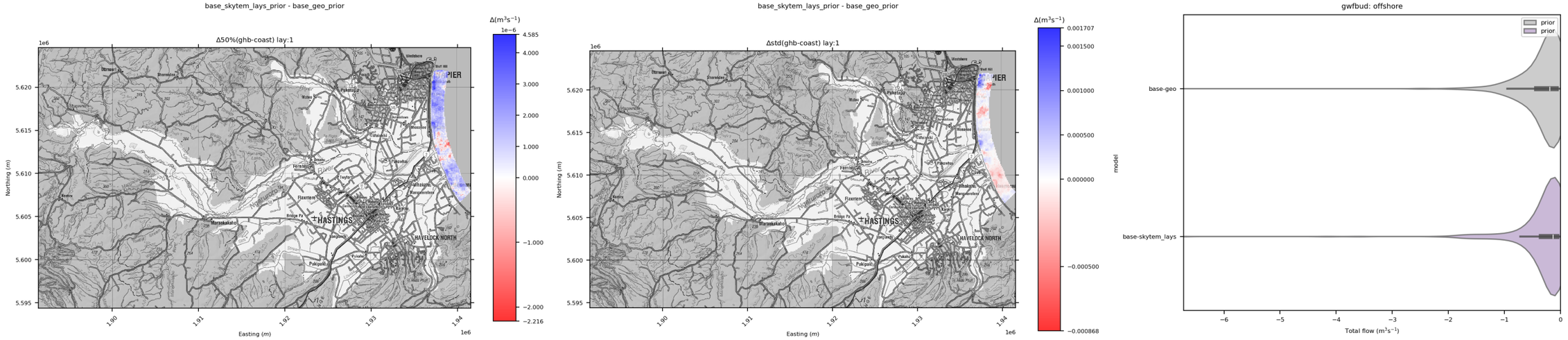

Figure 5.6 Change in simulated prior ensemble median (left) and standard deviation (middle) for offshore groundwater flow in model layer 1 for the updated model compared to the original model. Blue colours in left-hand plot indicate decreases in the ensemble median offshore flow (flow in the offshore direction is negative). For the middle plot, red colours indicate decreases in prior ensemble standard deviation (variance/uncertainty) in the updated model. (Right) Violin plots showing net offshore flow for prior ensembles from the original model (top) and updated model (bottom). Violin outlines estimate the kernel density of the ensembles; the inner boxplots show the interquartile range (IQR) and median (white bar), with whiskers extending to datapoints within 1.5 x IQR from the upper and lower quartiles.

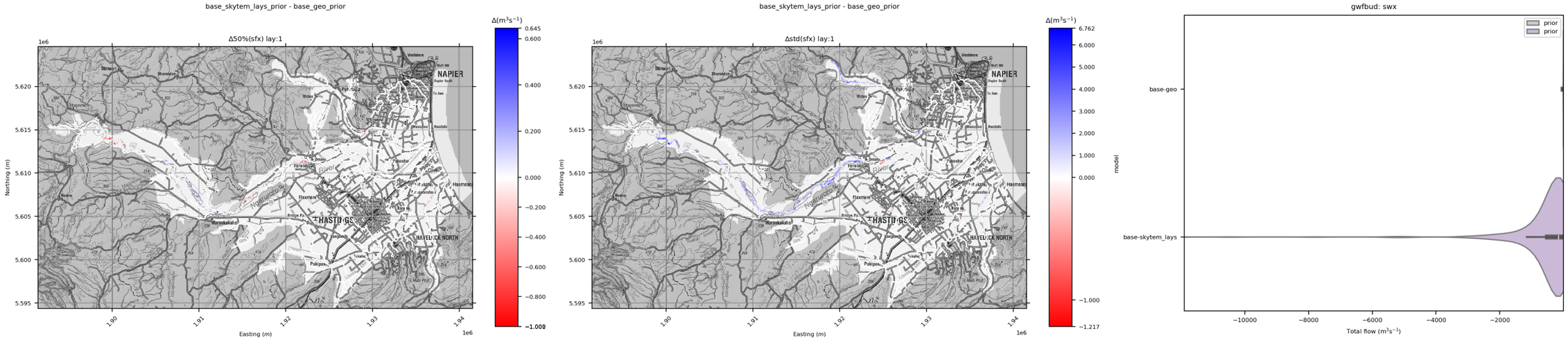

Figure 5.7 Change in simulated prior ensemble median (left) and standard deviation (middle) for surface-water–groundwater exchange (cell-by-cell) for the updated model compared to the original model. Blue colours in left-hand plot indicate increase in flow from groundwater to the stream (stream gain). For the middle plot, red colours indicate decreases in standard deviation (variance/uncertainty) captured in prior ensemble for the updated model. (Right) Violin plots showing prior ensemble simulated output distributions for net surface water groundwater exchange for the original model (top) and updated model (bottom). Negative values indicate net gain in surface water (i.e. loss of groundwater). Violin outlines estimate the kernel density of the ensembles; the inner boxplots shows the interquartile range (IQR) and median (white bar), with whiskers extending to datapoints within 1.5 x IQR from the upper and lower quartiles.

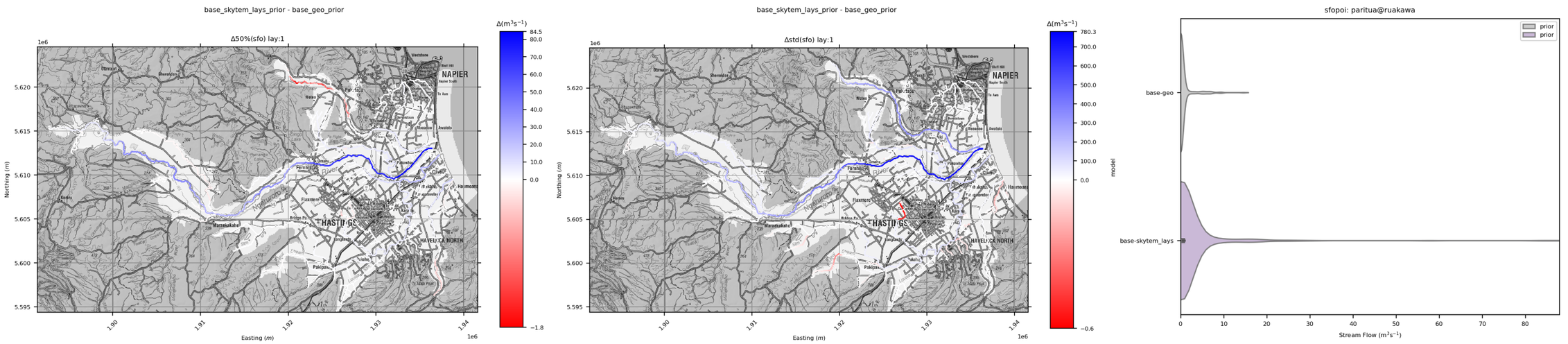

Figure 5.8 Change in simulated prior ensemble median (left) and standard deviation (middle) for stream flow for updated model compared to original model. Blue colours in left-hand plot indicate increase in flow. For the middle plot, red colours indicate decreases in standard deviation (variance/uncertainty) captured in prior ensemble for the updated model. (Right) Violin plots showing prior ensemble simulated output distributions for stream flow in the Paritua Stream at Ruakawa Road (Bridge Pā) for the original model (top) and updated model (bottom). Violin outlines estimate the kernel density of the ensembles; the inner boxplots shows the interquartile range (IQR) and median (white bar), with whiskers extending to datapoints within 1.5 x IQR from the upper and lower quartiles.

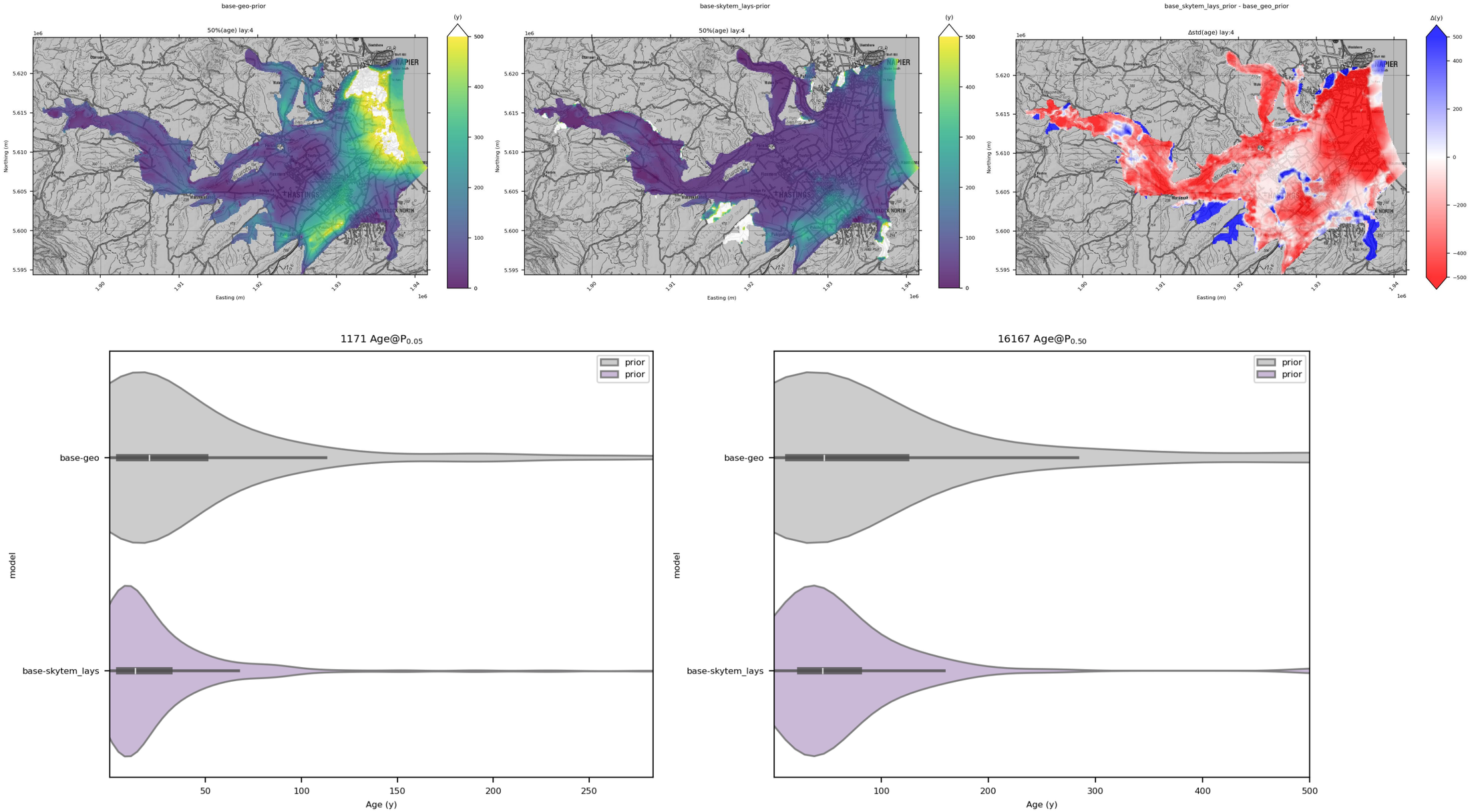

Figure 5.9 Simulated prior ensemble median for groundwater age in layer 4 for original model (top left) and updated model (top middle). The top-right image shows the change in standard deviation for the simulated age; red colours indicate decreases in standard deviation (variance/uncertainty) captured in prior ensemble for the updated model. Below, violin plots showing prior ensemble simulated output distributions for median groundwater age in two example wells (1171, Eastbourne St; left) and (16167, Lyndhurst Road; right) for the original model (top) and updated model (bottom). Violin outlines estimate the kernel density of the ensembles; the inner boxplots show the interquartile range (IQR) and median (white bar), with whiskers extending to datapoints within 1.5 x IQR from the upper and lower quartiles.